Tricritical Lifshitz point in the temperature-pressure-composition diagram for $(Pb_ySn_{1-y})_2P_2(Se_xS_{1-x})_6$ ferroelectrics

O. Andersson,[1] O. Chobal,[2] I. Rizak,[3] and V. Rizak[2]
[1]*Department of Physics, Umeå University, S-901 87 Umeå, Sweden*
[2]*Department of Solid State Electronics, Uzhhorod National University, 88000 Uzhhorod, Ukraine*
[3]*Department of Integrated Technologies of Aviation Manufacture, National Aerospace University of "KhAI," 61000 Kharkov, Ukraine*
(Received 25 June 2009; revised manuscript received 4 August 2009; published 11 November 2009)

The heat capacity of $Sn_2P_2S_6$ ferroelectric crystals has been measured under quasihydrostatic pressures up to 0.7 GPa. The analysis of the heat-capacity and literature data for the birefringence shows that the tricritical point of $Sn_2P_2S_6$ is in the 0.20–0.25 GPa range. Moreover, in the approximation of a linear change in the free-energy expansion coefficients, with respect to concentration and pressure, thermodynamic trajectories have been constructed for $(Pb_ySn_{1-y})_2P_2(Se_xS_{1-x})_6$ solid solutions. We have thereby identified the region of the *T-p-y-x* diagram for $(Pb_ySn_{1-y})_2P_2(Se_xS_{1-x})_6$ showing the tricritical Lifshitz point.

DOI: 10.1103/PhysRevB.80.174107 PACS number(s): 64.60.Kw, 62.50.−p, 65.40.Ba, 68.35.Rh

I. INTRODUCTION

It is well known that besides first- and second-order phase transitions (PT) and normal critical points, higher-order critical points may arise in some systems.[1] Two such are the tricritical point (TCP) and the Lifshitz point (LP). A TCP is characterized by a change in order of a transition from second to first, or vice versa, for a direct transition between two phases, where one belongs to a symmetry subgroup of the other.[2] In a ferroelectric system such as $Sn_2P_2S_6$, these are typically ferroelectric (low-symmetry) and paraelectric (high-symmetry) phases. Another high-order critical point, a LP (Ref. 3) is a special case of a triple point. It separates a region with a second-order transition between a high-symmetry (e.g., paraelectric) and a low-symmetry (e.g., ferroelectric) commensurate phase from one where this transformation occurs via an incommensurate (IC) phase. That is, the three phase boundaries between these phases join at the LP. Only a few systems have been found that show both a TCP and a LP. By simultaneously varying properties such as temperature (T), pressure (p), and composition (x) for those systems, it is possible to follow the TCP and the LP in a (T-p-x) diagram and explore if these merge in a higher-order critical point, i.e., in a tricritical Lifshitz point (TCLP),[4] which is the subject of this study.

The static and dynamical properties of the lattice in the ferroelectric $(Pb_ySn_{1-y})_2P_2(Se_xS_{1-x})_6$ semiconductors have previously been studied.[5–7] The analysis of these shows that compounds of the type $(Pb_ySn_{1-y})_2P_2(Se_xS_{1-x})_6$ are the most perspective materials to reach a TCLP.[8,9] The aim of this work was to specify the coordinates of the TCLP on the basis of direct studies of the heat capacity for $Sn_2P_2S_6$ crystals under compression and an analysis of the available results on birefringence and spontaneous polarization in $(Pb_ySn_{1-y})_2P_2(Se_xS_{1-x})_6$ solid solutions.

II. EXPERIMENTAL DETAILS

The transient hot-wire method was used to measure the heat capacity per unit volume ρc_p, where c_p is the isobaric specific-heat capacity and ρ is the mass density. This method has previously been described in detail in Refs. 10 and 11. Briefly, the hot-wire probe was a nickel wire, 0.1 mm in diameter and 40 mm long, placed horizontally in a ring of constant radius within a ~15 mm deep and 37 mm internal diameter Teflon container with a tight sealing 5 mm Teflon cover. The Teflon cell is closely fitted inside a piston-cylinder-type apparatus of 45 mm internal diameter and the whole assembly is transferred to a hydraulic press that supplies the load. To determine ρc_p, the wire probe embedded in the sample (32 g of polycrystalline $Sn_2P_2S_6$ grown by the gas-transport reaction technique[12]) was heated by the 1.4 s duration electric pulse of almost constant power, yielding a temperature rise of about 3.5 K. The temperature rise of the wire as a function of time was calculated by using its electrical resistance-temperature relation, i.e., the wire works as both heater and sensor for the temperature rise. The analytical solution for the temperature rise with time was fitted to the data points for the hot-wire temperature rise with an inaccuracy of ~5% in ρc_p, and a standard deviation an order of magnitude smaller.

The temperature of the piston cylinder could be controlled by varying the power to an electrical resistance heater placed on the cylinder. For measurements below room temperature, the vessel was cooled using liquid nitrogen. The temperature of the specimen was measured using an internal Chromel Alumel thermocouple, which had been calibrated to within ±0.2 K of a commercial silicon diode thermometer with an accuracy of 10 mK. The pressure fluctuation during isobaric measurements, which was also controlled using a proportional-integral-derivative controller, was less than ~1 MPa.

III. RESULTS AND DISCUSSION

The results for ρc_p of $Sn_2P_2S_6$ crystals for pressures in the 0.1–0.7 GPa range are depicted in Fig. 1. As shown in Fig. 1, an anomaly, associated with a phase transition, shifts toward lower temperatures with increasing pressure. (The heat-capacity anomalies are slightly blurred, possibly due to temperature gradients in the Teflon sample cell.) This agrees well with the results of optical studies and dielectric perme-

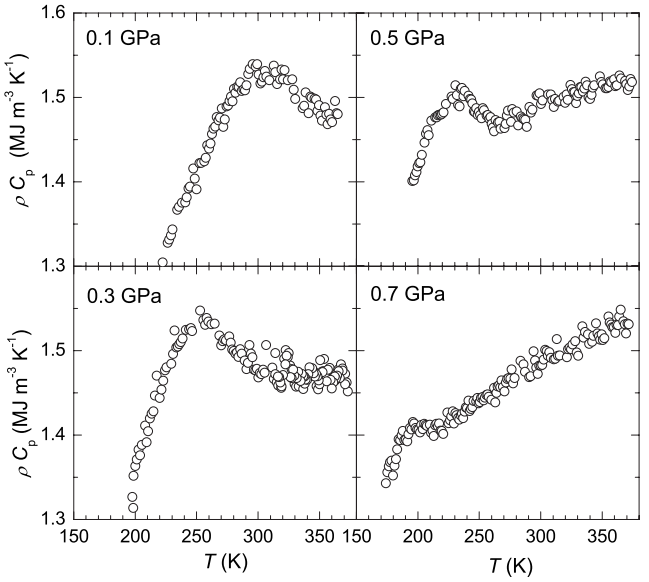

FIG. 1. Heat capacity per unit volume plotted against temperature for $Sn_2P_2S_6$ crystals in the vicinity of phase transition at pressure in the 0.1–0.7 GPa range.

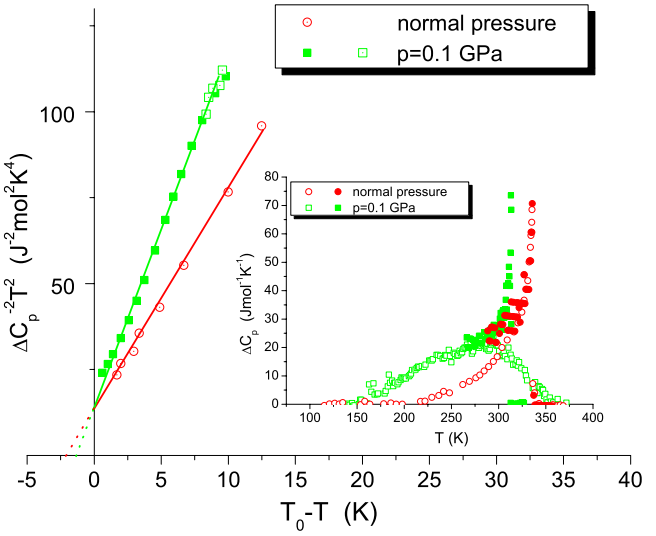

FIG. 2. (Color online). Temperature dependences $(\Delta C_p/T)^{-2}$ in the ferroelectric phase of $Sn_2P_2S_6$ crystals at normal pressure and at 0.1 GPa. Inset—the temperature behavior of the excess heat capacity (open symbols—the measured heat capacity and dark symbols—the birefringence derivative).

ability measurements.[13] The transition coordinates determined from the isobaric results of ρc_p are superimposed on the phase boundaries within the limits of experimental error. At isobars below the pressure for the LP $[p_{LP}=0.19$ GPa (Ref. 13)], the ρc_p anomalies agree with the established phase boundary between the ferroelectric and paraelectric phases whereas at pressures above these agree with the boundary between the ferroelectric and incommensurate phases. Thus, the transition between the paraelectric phase and the incommensurate phase (at $p>p_{LP}$) cannot be resolved in the data for ρc_p, which indicates that associated change in ρc_p is small and within the imprecision of the method.

We begin by analyzing the excess heat capacity ΔC_p, which in terms of the mean-field theory is determined by[14]

$$\Delta C_p(T) = \frac{T}{2\rho C_K^2}\left[\beta^2 - \frac{4(T-T_0)\gamma}{C_K}\right]^{-1/2}, \qquad (1)$$

where T_0 is the PT temperature, ρ is the substance density, C_K is the Curie-Weiss constant, and β and γ are the coefficients of the free-energy Φ expansion,

$$\Phi(p,T,\eta) = \Phi_0(p,T) + \frac{\alpha}{2}\eta^2 + \frac{\beta}{4}\eta^4 + \frac{\gamma}{6}\eta^6 + \frac{\delta}{2}\left(\frac{d\eta}{dz}\right)^2 + \frac{g}{2}\left(\frac{d^2\eta}{dz^2}\right) + \cdots, \qquad (2)$$

where η is the order parameter. From Eq. (1) it follows that the quantity $K=\beta^2/4\alpha\gamma T_0$, which determines the phase-transition proximity to the tricritical point,[14,15] can be determined from the linear plot of $(\Delta C_p/T)^{-2}$ vs $(T-T_0)$.

Figure 2 presents the experimental results for the excess heat capacity (ΔC_p) of $Sn_2P_2S_6$ ferroelectrics at normal (atmospheric) pressure and at 0.1 GPa pressure in the vicinity of the phase transition. The regular part of the heat capacity was obtained by interpolation of the heat capacity for the paraelectric phase and that for the ferroelectric phase far from the PT using a third-order polynomial, and then extracted from the measured values. As mentioned above, the heat-capacity anomalies at high pressures are blurred. To improve the analysis, we have therefore also used the temperature derivative of the birefringence, which is proportional to the excess heat capacity.[16,17] The algorithm for the use of the birefringence is as follows. The birefringence derivative calculated from normal pressure data was scaled to superimpose on the heat capacity measured under normal pressure using adiabatic calorimetry.[8] Subsequently, the same scaling parameters were used to calculate the heat capacity at 0.1 GPa from the birefringence data at 0.1 GPa.[18] The results above the transition were included in the fit of the third-order polynomial to obtain the regular part of the heat capacity and those below were combined with the experimental heat capacity at 0.1 GPa. As shown by the inset of Fig. 2, the two data sets for ΔC_p agree well below the transition, which verifies the validity of the scaling procedure. The results plotted as $(\Delta C_p/T)^{-2}$ vs (T_0-T) are well described by linear functions (Fig. 2), and their intersection with the abscissa axis gives the value for $\beta^2/4\alpha\gamma(=KT_0)$. Since this quantity is a measure of the PT proximity to the TCP, the results in Fig. 2 show that an increase in pressure to 0.1 GPa moves the PT closer to the TCP.

For a more exact determination of the TCP for $Sn_2P_2S_6$, we have calculated $\Delta C_p(T)$ from birefringence data at pressures up to ~0.16 GPa (Ref. 18) using the same scaling procedure as described above. As shown in Fig. 3(a), the results for K, which were derived from the plots of $(\Delta C_p/T)^{-2}$ vs (T_0-T), decreases linearly with increasing pressure. The linear extrapolation intersects the abscissa axis at $p\approx 0.23$ GPa, which thus corresponds to the pressure for the TCP of $Sn_2P_2S_6$ ferroelectrics. Moreover, this result

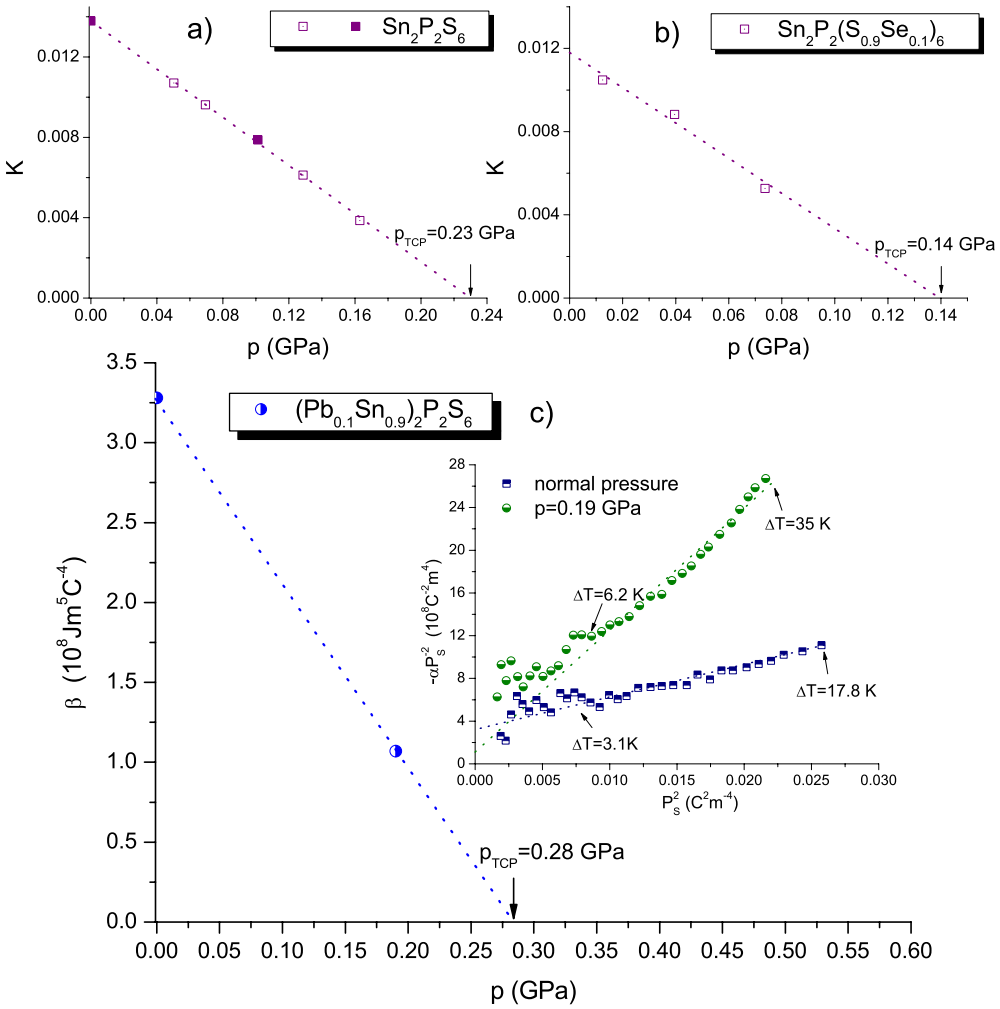

FIG. 3. (Color online). Baric dependences of K and β values for $(Pb_ySn_{1-y})_2P_2(Se_xS_{1-x})_6$ solid solutions. (Open symbols—the birefringence data, dark symbols—the heat-capacity data, and half-closed symbols—the spontaneous polarization data). The inset shows $-\frac{\alpha}{P^2}$ plotted against the polarization squared P^2 measured at different temperatures and pressures.

shows that a direct PT from the paraelectric phase to the ferroelectric phase at pressures exceeding 0.23 GPa would be a first-order transition. However, since the IC phase intervenes at pressures above $p_{LP}=0.19$ GPa,[13] the PT cannot be observed experimentally and is thus virtual at 0.23 GPa.

To proceed further, we use high-pressure data for birefringence[19] and spontaneous polarization[20,21] to analyze the PT's in $(Pb_ySn_{1-y})_2P_2S_6$ and $Sn_2P_2(Se_xS_{1-x})_6$ solid solutions from the viewpoint of their proximity to the TCP. In particular, for $Sn_2P_2(Se_{0.1}S_{0.9})_6$ the analysis of the birefringence derivative, carried out according to the algorithm described above for $Sn_2P_2S_6$, indicates a virtual TCP at $p \approx 0.14$ GPa [Fig. 3(b)].

In accordance with thermodynamical theory, the equation of state for a ferroelectric crystal, with polarization P being the order parameter, is defined by the following expression:[22]

$$E = \alpha P + \beta P^3 + \gamma P^5 + \cdots, \tag{3}$$

where E is the electric field strength. As follows from Eq. (3), in absence of an electric field, a plot of $-\frac{\alpha}{P^2}$ vs P^2 at different temperatures must give a linear dependence. In this case, the point of intersection of this straight line with the ordinate axis defines the coefficient β while its slope defines γ.[22] The analysis of the results of spontaneous polarization in $(Pb_{0.1}Sn_{0.9})_2P_2S_6$ proves the Landau's theory for the ferroelectrics under study in a quite wide temperature range close to T_0 [inset of Fig. 3(c)]. The deviations from the linear law observed in the inset of Fig. 3(c) are probably explained by the error in measuring the spontaneous polarization close to the PT. Extrapolation of $\beta(p)$ for $(Pb_{0.1}Sn_{0.9})_2P_2S_6$ into the range $\beta<0$ [Fig. 3(c)] indicates that the PT approaches the TCP but due to the IC phase it cannot be studied at $p > 0.28$ GPa.

In summary, the analysis of the results of our studies on $(Pb_ySn_{1-y})_2P_2S_6$ and $Sn_2P_2(Se_xS_{1-x})_6$ crystals have allowed us to adjust and supplement the diagram of their "thermodynamic trajectory" (see Ref. 8).

We have constructed a concentration thermodynamic trajectory for $Sn_2P_2(Se_xS_{1-x})_6$ based on literature data.[8,23] Moreover, the baric thermodynamic trajectory for Sn_2P_2S was constructed using the values for the LP ($p_{LP}=0.19$ GPa, $\delta=0$) (Ref. 13) and the virtual TCP ($p_{TCP}=0.23$ GPa, $\beta=0$). As described above, the pressures of the

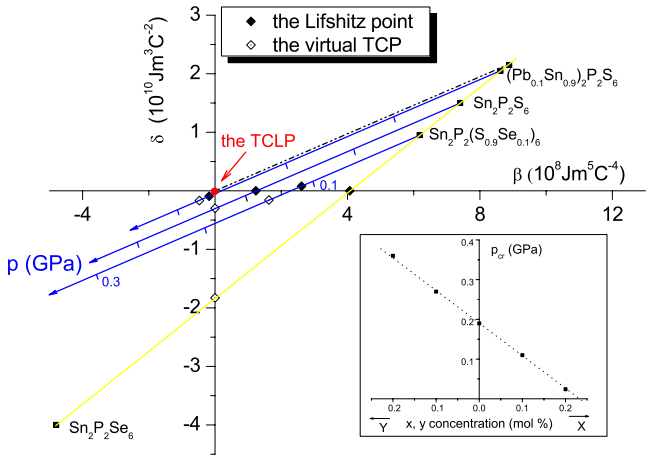

FIG. 4. (Color online). Concentration and baric "thermodynamic trajectory" in the δ-β plane for $(Pb_ySn_{1-y})_2P_2(Se_xS_{1-x})_6$ ferroelectrics. Inset—concentration dependence of the "critical" pressure (p_{cr}) that corresponds to the PT line splitting (Refs. 21 and 24).

TCPs were obtained from data for $C_p(T)$. The analysis of the experimental data in the mean-field approximation for $Sn_2P_2S_6$ crystals shows that under hydrostatic pressurization first the Lifshitz point $[\alpha(T,p)=0;\ \delta(T,p)=0]$ is reached and, subsequently, the virtual TCP $[\alpha(T,p)=0;\ \beta(T,p)=0]$. This means that the baric thermodynamic trajectory of $Sn_2P_2S_6$ ferroelectrics passes near the concentration trajectory for those of $Sn_2P_2(Se_xS_{1-x})_6$ solid solutions (Fig. 4). Based on the pressure shifts of the phase line with changing concentration[21,24] (see inset of Fig. 4) as well as the TCP coordinates obtained here for the $(Pb_ySn_{1-y})_2P_2S_6$ and $Sn_2P_2(Se_xS_{1-x})_6$ solid solutions, it is reasonable to assume that the replacements S→Se and Sn→Pb result in a parallel shift of the baric thermodynamic trajectory for $Sn_2P_2S_6$. We have thus used identical scales for the pressure axis of the three studied systems ($x=y=0$, $x=0.1$ and $y=0$, $x=0$ and $y=0.1$). The thermodynamic trajectories constructed under the assumption of linear changes in the free-energy expansion coefficients, with respect to concentration and pressure, describe fairly well the coordinates of the experimental critical points. The discrepancies can, at least partly, be explained by the use of a linear concentration dependence of the critical pressure.[21,24] The linear extrapolation to normal pressure yields the Lifshitz point at $x=0.23$ in $Sn_2P_2(Se_xS_{1-x})_6$ solid solutions whereas the array of the experimental data[5] indicates reaching the Lifshitz point at 0.28 mol % Se concentration.

As shown in Fig. 4, it is possible to reach the TCLP at 0.28 GPa in $(Pb_{0.12}Sn_{0.88})_2P_2S_6$ crystals. We can also estimate the temperature of the TCLP based on the T-p-y phase diagrams of $(Pb_ySn_{1-y})_2P_2S_6$ solid solutions.[21] According to the phase diagrams,[21] the paraelectric to ferroelectric PT in $(Pb_{0.12}Sn_{0.88})_2P_2S_6$ crystals occurs at $T_0=295$ K at atmospheric pressure. In linear approximations, the changes in the transition temperature with pressure, (dT_0/dp), for $(Pb_ySn_{1-y})_2P_2S_6$ solid solutions is $dT_0/dp=-251$ K/GPa for $y=0.12$, as far as according to experimental data[21] at $y=0.1$, $dT_0/dp=-250$ K/GPa and at $y=0.2$, $T_0/dp=-255$ K/GPa. At 0.28 GPa, i.e., at the estimated pressure for the TCLP of $(Pb_{0.12}Sn_{0.88})_2P_2S_6$, the PT temperature T_0 is the same as that for the TCLP, which yields $T_{TCLP}=T_0=225$ K using the value for dT_0/dp.

IV. CONCLUSIONS

The results obtained here for $(Pb_ySn_{1-y})_2P_2(Se_xS_{1-x})_6$ solid solutions show that the tricritical Lifshitz point occurs at about $T=225$ K; $p=0.28$ GPa; $x=0$; $y=0.12$. This gives a possibility of comprehensive studies of such higher-order critical point under easily realized experimental conditions.

[1] T. S. Chang, G. F. Tuthill, and H. E. Stanley, Phys. Rev. B **9**, 4882 (1974).
[2] I. I. Novikov, High Temp. **40**, 352 (2002).
[3] R. M. Hornreich, M. Luban, and S. Shtrikman, Phys. Rev. Lett. **35**, 1678 (1975).
[4] J. F. Nicoll, G. F. Tuthill, T. S. Chang, and H. E. Stanley, Phys. Lett. A **58**, 1 (1976); J. F. Nicoll, T. S. Chang, and H. E. Stanley, Phys. Rev. A **13**, 1251 (1976).
[5] D. G. Semak, V. M. Rizak, and I. M. Rizak, *Photothermostructural Transformation of Chalcogenides* (Zakarpattya, Uzhhorod, Ukrainian, 1999).
[6] V. M. Rizak, I. M. Rizak, and D. G. Semak, *Functional Chalcogenide Semiconductors* (Zakarpattya, Uzhhorod, Ukrainian, 2001).
[7] Yu. M. Vysochanskii, T. Janssen, R. Currat, R. Folk, J. Banys, J. Grigas, and V. Samulionis, *Phase Transitions in Phosphorous Chalcogenide Ferroelectrics* (Vilnius University, Vilnius, 2006).
[8] Yu M. Vysochanski, M. M. Maior, V. M. Rizak, V. Yu. Slivka, and M. M. Khoma, Zh. Eksp. Teor. Fiz. **95**, 1355 (1989) [Sov. Phys. JETP **68**, 782 (1989)].
[9] Yu. Tyagur, Ferroelectrics **345**, 91 (2006).
[10] B. Håkansson, P. Andersson, and G. Bäckström, Rev. Sci. Instrum. **59**, 2269 (1988).
[11] O. Andersson and A. Inaba, Phys. Chem. Chem. Phys. **7**, 1441 (2005).
[12] C. D. Carpentier and R. Nitsche, Mater. Res. Bull. **9**, 401 (1974).
[13] Yu. I. Tyagur and E. I. Gerzanich, Kristallografiya **29**, 957 (1984) Sov. Phys. Crystallogr. **29**, 563 (1984)].
[14] B. A. Strukov and A. P. Levanyuk, *Fizicheskie Osnovy Segnetoelektricheskikh Yavleniî v Kristallakh* (Nauka, Moscow, 1995) (reprinted by Springer, Berlin, 1998].
[15] Y. Won Song, J. C. Kim, I. K. You, and B. A. Strukov, Mater. Res. Bull. **35**, 1087 (2000).
[16] J. Ferre and G. A. Gehring, Rep. Prog. Phys. **47**, 513 (1984).
[17] N. R. Ivanov, A. P. Levanyuk, S. A. Minyukov, I. Kroupa, and I. Fousek, J. Phys.: Condens. Matter **2**, 5777 (1990).
[18] R. Kabal and P. Guranich, Visnyk Lviv Univ., Ser. Physic. **36**, 158 (2003).
[19] A. G. Slivka, P. P. Guranich, R. V. Kabal, and E. I. Gerzanich,

Ukr. J. Phys. Opt **2**, 179 (2001)
[20] V. S. Shusta, E. I. Gerzanich, A. G. Slivka, and P. P. Guranich, Fiz. Tverd. Tela (Leningrad) **31**, 308 (1989) [Sov. Phys. Solid State **31**, 2016 (1989)].
[21] V. S. Shusta, E. I. Gerzanich, A. G. Slivka, P. P. Guranich, and V. A. Bobela, Ferroelectrics **145**, 61 (1993).
[22] E. V. Sidnenko and V. V. Gladkiy, Kristallografiya **17**, 978 (1972) [Sov. Phys. Crystallogr. **17**, 861 (1973)]; K. S. Aleksandrov and I. N. Flerov, Fiz. Tverd. Tela. (Leningrad) **21**, 327 (1979) Sov. Phys. Solid State **21**, 195 (1979)].
[23] Yu. M. Vysochanskii, M. M. Maior, V. M. Rizak, V. Yu. Slivka, S. I. Perechinskii, and M. M. Khoma, Izv. Akad. Nauk SSSR, Ser. Fiz. **54**, 677 (1990) [Bull. Acad. Sci. USSR, Phys. Ser. **54**, 75 (1990)].
[24] A. G. Slivka, E. I. Gerzanich, P. P. Guranich, and V. S. Shusta, Ferroelectrics **103**, 71 (1990).